

# **Lake area constraints on past hydroclimate in the western United States: Application to Pleistocene Lake Bonneville**

Daniel E. Ibarra<sup>1, \*</sup>, Jessica L. Oster<sup>2</sup>, Matthew J. Winnick<sup>3</sup>, Jeremy K. Caves Rugestein<sup>4</sup>,  
Michael P. Byrne<sup>5</sup>, and C. Page Chamberlain<sup>1</sup>

<sup>1</sup> Dept. of Geological Sciences, Stanford University, 450 Serra Mall, Building 320, Stanford, CA 94305-2115

<sup>2</sup> Dept. of Earth and Environmental Sciences, Vanderbilt University, 5726 Stevenson Center; 7<sup>th</sup> Floor, Nashville, TN 37240, USA

<sup>3</sup> Dept. of Geosciences, 611 North Pleasant Street, 233 Morrill Science Center, University of Massachusetts Amherst, Amherst, MA 01003-9297, USA

<sup>4</sup> Dept. of Earth Sciences, ETH Zürich, NO E61 Sonneggstrasse 5, 8092 Zürich, Switzerland

<sup>5</sup> Space and Atmospheric Physics Group, Dept. of Physics, Imperial College London, Prince Consort Road, London SW7 2AZ, UK

\* Corresponding Author: [danieli@stanford.edu](mailto:danieli@stanford.edu)

Extended abstract manuscript submitted to the Utah Geological Society Miscellaneous Publications as a contribution to the 2018 Lake Bonneville Geology Conference Proceedings Volume

## **ABSTRACT**

Lake shoreline remnants found in basins of the western United States reflect wetter conditions during Pleistocene glacial periods. The size distribution of paleolakes, such as Lake Bonneville, provide a first-order constraint on the competition between regional precipitation delivery and evaporative demand. In this contribution we downscale previous work using lake mass balance equations and Budyko framework constraints to determine past hydroclimate change for the Bonneville and Provo shoreline extents of Lake Bonneville during the last glacial cycle. For the Bonneville basin we derive new relationships between temperature depression and precipitation factor change relative to modern. These scaling relationships are combined with rebound-corrected estimates of lake area and volume and macrofossil-derived surface temperatures to make quantitative estimates of precipitation and water residence times for the lake. For the Bonneville shoreline (~1552 m) we calculate that, prior to spillover to the Snake River drainage, precipitation rates were ~1.37 times modern, with a water residence time of ~185 years. For the Provo shoreline (1444 m), during the period of steady-state spillover, we calculate that precipitation rates were at least 1.26 times modern, with a residence time of ~102 years. These calculations suggest minimal difference in the hydrologic regime between the Bonneville shoreline highstand and the Provo shoreline stillstand during the last glacial termination. These estimates of hydroclimate scaling relationships differ in sensitivity with previous hydrologic modeling for Lake Bonneville and are complementary to those recently derived from glacier mass balance modeling from the Wasatch Mountains.

## INTRODUCTION AND METHODOLOGY

The size of pluvial lakes in terminally draining basins of the western United States indicate a substantially different landscape during Pleistocene glacial periods. Building on the seminal work of G.K. Gilbert (1890) and J.C. Russell (1885), shoreline mapping and compilations of late Pleistocene lake surface areas in the western United States (e.g., Hubbs and Miller, 1948; Mifflin and Wheat, 1979; Williams and Bedinger, 1984; Reheis, 1999a; Orme, 2008; Grayson, 2011) has led to estimates of hydroclimate based on steady-state mass balance assumptions related to observed lake areas (e.g., Mifflin and Wheat, 1979; Hostetler and Benson, 1990; Reheis, 1999b; Broecker, 2010; Matsubara and Howard, 2009; Munroe and Laabs, 2013; Reheis and others, 2014; Ibarra and others, 2014; 2018; Barth and others, 2016). Geologic observations of shorelines or outcrop extent from ancient lake systems thus serve as constraints for to provide quantitative paleoclimate reconstructions for comparison to climate model experiments (e.g., Ibarra et al., 2014; Oster et al., 2015; Barth et al., 2016; Lora et al., 2017).

One such relationship, derived from the steady-state water balance assumption, is for the area of the lake ( $A_L$ ) to the area of the basin ( $A_B$ ) (Hudson and Quade, 2013; Ibarra and others, 2018):

$$\frac{A_L}{A_B} = \frac{P-ET}{E_L-P+Pk_{run}} = \frac{Pk_{run}}{E_L-P+Pk_{run}} \quad (1),$$

where:

$A_L$  and  $A_B$  = the areas of the lake and basin, respectively (km<sup>2</sup>).

$P$  = the basin average precipitation (mm/year).

$ET$  = the tributary average evapotranspiration (mm/year).

$E_L$  = the lake average evaporation (mm/yr).

$k_{run}$  = the runoff ratio of the subaerial portion of the watershed (i.e.,  $P-ET = Pk_{run}$ ), including both groundwater and riverine runoff into the basin.

The relationship between precipitation and runoff is non-linear across climate states, and thus necessitates increased proportional runoff (higher  $k_{run}$ ) with increased precipitation. To impose this non-linear relationship, we use the Budyko framework (Budyko, 1974; Fu, 1981; Broecker, 2010; Roderick and others, 2014; Greve and others, 2015), where  $k_{run}$  is determined, using the Fu (1981) formulation, as:

$$1 - k_{run} = \frac{ET}{P} = 1 + \frac{E_p}{P} - \left[ 1 + \left( \frac{E_p}{P} \right)^\omega \right]^{\frac{1}{\omega}} \quad (2),$$

where:

$E_p$  = potential evapotranspiration, the liquid water equivalent of the net downward radiation at the Earth surface derived from energy fluxes (Roderick and others, 2014; Ibarra and others, 2018).

$\omega$  = a free parameter that integrates the hydroclimatic properties of a watershed or basin (Fu, 1981; Greve and others, 2015).

The global average  $\omega$  value is  $\sim 2.6$  (Roderick and others, 2014; Greve and others, 2015). Recent work has shown that more complex, spatially explicit hydrologic modeling of Pleistocene lakes follow precipitation-runoff relationships imposed by the Budyko framework (Matsubara and Howard, 2009; Barth and others, 2016), justifying this scaling approach for steady-state calculations.

In this contribution, we use the methods outlined by Ibarra and others (2018) to analyze the distribution of the precipitation and energy fields from the gridded North American Regional Reanalysis dataset (NARR). We downscale the results presented by Ibarra and others (2018) for the Bonneville basin, defined by the NARR grid cells (resolution of NARR is 32 km,  $n=201$  grid cells) spanning the region (37.5 to 43 °N, 114.5 to 110.5 °W) and present results based on the median change in lake area. We have confirmed that the average NARR precipitation fields (1979 to present) agree well with the 30-year normal PRISM precipitation dataset (1981 to 2010) and long-term weather station data archived by the Western Regional Climate Center. Lake evaporation ( $E_L$ ) is calculated using the Priestley-Taylor equation and an  $E_p$  versus temperature scaling of 1.6%/K (Ibarra and others, 2018). To calibrate the lake area scaling relationships specifically for Lake Bonneville we lower the Budyko  $\omega$  value to 2.465, which is calibrated to the total modern lake and seasonal playa lake surface area (8,924 km<sup>2</sup>, modern  $A_L/A_B = 6.65\%$ ), which includes the Great Salt Lake, Bear Lake, the Bonneville Salt Flats and other seasonal playa lakes as compiled in Ibarra and others (2018).

For the latest glacial Provo and Bonneville shorelines we use rebound corrected lake area and volume estimates determined by Adams and Bills (2016), and temperature depression estimates based on macrofossil assemblages determined by Harbert and Nixon (2018) (see Table 1). Use of the non-rebounded corrected values would result in underestimates in both precipitation and lake residence times. We note that the Bonneville shoreline lake area and volume estimate reported by Adams and Bills (2016) agree well with new high-precision

differential GPS measurements reported by Chen and Maloof (2017) (see also Currey and others, 1982; Bills and others, 2002; 2016). All contours and scaling relationships shown are the median change in precipitation and temperature (for details see Ibarra and others, 2018), intended to represent the basin average change in hydroclimate necessary to explain the observed lake areas. Medians of the calculated  $A_L/A_B$  distributions are used due to the non-normal distribution in modern precipitation and energy fluxes used for the scaling analysis. We report uncertainty ranges on our estimates, where the uncertainty reflects the full range of temperature estimates, and is asymmetric due to the Budyko scaling relationship and the non-normal distribution in modern precipitation and energy fluxes.

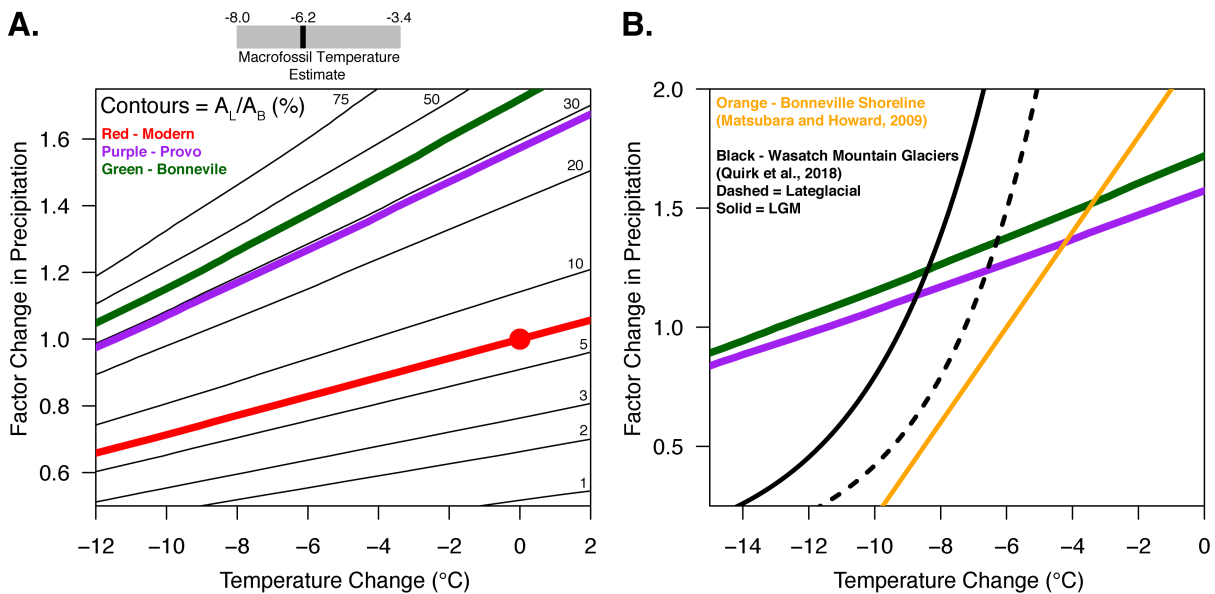


**Figure 1. Hydroclimate change inferred from Lake Bonneville shoreline areas. (A)** Contoured basin area-normalized lake area based on changes in precipitation and temperature over the Bonneville Basin (37.5 to 43 °N, 114.5 to 110.5 °W). Colored lines denote the modern (red), Provo shoreline (purple) and Bonneville shoreline (dark green). Macrofossil temperature depression estimates are from Harbert and Nixon (2018). Note that the black contours are not linear. **(B)** Comparison of lake area scaling relationships with previous temperature vs. precipitation estimates from hydrologic modeling of the Bonneville shoreline (Matsubara and Howard, 2009) and glacier mass balance modeling from Big Cottonwood Canyon in the Wasatch Mountains (UT) (Quirk and others, 2018), located on the eastern edge of Lake Bonneville. Note the axes difference between panels A and B.

## **RESULTS AND DISCUSSION**

The results of our downscaled sensitivity analysis for Bonneville are displayed in Figure 1A and reported in Table 1. Solved for all combinations assuming a uniform temperature depression and factor change in precipitation over the basin, we plot the calculated precipitation factor change as a function of temperature depression needed to maintain a given lake area (expressed as  $A_L/A_B$ ; black contours in Figure 1A). The colored contours on Figure 1A represent the Bonneville, Provo and modern surface area estimates.

Combining the temperature depression and lake area estimates (see above and Table 1) for the Bonneville shoreline surface area prior to spill over into the Snake River (~18.5 ka), we calculate precipitation rates that were ~1.37 (+0.15/−0.10) times modern with a water residence time of 185 (+13/−16) years. This estimate is comparable but higher than the Paleoclimate Modeling Intercomparison Project (PMIP) 2 and 3 Last Glacial Maximum (LGM;  $n = 15$ ) ensemble average of 1.17 ( $\pm 0.47$ ,  $1\sigma$ ) for Lake Bonneville determined previously by Oster and others (2015), though we note that the best performing PMIP3 models ( $n = 5$ ) suggest minimal change in precipitation ( $1.02 \pm 0.19$ ) relative to modern. Our estimates of precipitation change for the LGM are higher than the central estimates from data to the west from Newark Valley (1.14 times modern, +0.15/−0.59) and Diamond Valley (0.97 times modern, +0.10/−0.51), derived from uranium-series systematics in soil opal (Maher and others, 2014; see their Table 2), but lower than estimates from lake balance modeling of Jakes Lake (~1.9 times modern produced by Barth and others (2016).

Similarly, for the Provo shoreline, we calculate a minimum precipitation factor change of 1.26 (+0.13/−0.09) times modern, and a water residence time of 102 (+7/−9) years. We note that minimal change in precipitation over the Bonneville region between the LGM and ~15.5 ka is simulated by the TraCE climate model simulation of the last 22 kyrs (Lora and others, 2017; see their Figure 4). Given ~2.5 kyr of stable shoreline development and continual overflow (Miller and others, 2013; Oviatt, 2015), this precipitation estimate is likely a minimum value considering the balance-filled nature of the Lake Bonneville system.

**Table 1.** Modeling inputs and results for Lake Bonneville.

Lake Stage	Lake Area [km <sup>2</sup> ] <sup>1</sup>	Volume [km <sup>3</sup> ] <sup>1</sup>	P/P <sub>M</sub> vs. $\Delta T$ relationship <sup>2</sup>	Precipitation Factor Change	Water Residence Time (yr)
<b>Bonneville</b>	52,110 (A <sub>L</sub> /A <sub>B</sub> = 38.85%)	10,420	P/P <sub>M</sub> = 1.711 + 0.056× $\Delta T$	1.37 (+0.15/−0.10)	185 (+13/−16)
<b>Provo</b>	38,150 (A <sub>L</sub> /A <sub>B</sub> = 28.44%)	5,290	P/P <sub>M</sub> = 1.572 + 0.050× $\Delta T$	> 1.26 (+0.13/−0.09)	102 (+7/−9)

<sup>1</sup> Rebound corrected lake volume and areas determined by Adams and Bills (2016).

<sup>2</sup> P/P<sub>M</sub> = precipitation factor change;  $\Delta T$  = temperature change relative to modern. Linear relationships are approximate based on linear regression fit to contours in Figure 1.

**Modeling assumptions:** Budyko parameter,  $\omega = 2.465$  (calibrated to total modern lake and playa areas; 8,924 km<sup>2</sup>); Total basin area = 134,131 km<sup>2</sup>; Residence time calculation assumes modern precipitation rate of 338 mm/yr (NARR median; comparable to PRISM value of 344 mm/yr); median temperature depression of −6.2 (−8.0 to −3.4 °C) based on filtering of macrofossil assemblage calculation from Harbert and Nixon (2018) for all deglacial and LGM locations (n=13) near Lake Bonneville; and temperature vs. potential evapotranspiration scaling of 1.6%/°C (Ibarra and others, 2018). Basin and modern lake/playa areas are from data tables in Ibarra and others (2018).

The residence of time of water in Lake Bonneville for the Bonneville and Provo shorelines place useful constraints on oxygen isotope measurements of sediments or shoreline tufa, though other geochemical systems, such as trace elements, are typically decoupled from water residence times. Our residence time calculations (Table 1) place minimum bounds on the timescale that oxygen isotope timeseries from cores or other high-resolution records could record rapid (sub-kyr) changes in climate (e.g., Dansgaard–Oeschger or Heinrich events) occurring within glacial-interglacial cycles (e.g., Benson and others, 1990; Oviatt and others, 1994; McGee and others, 2012; Ibarra and Chamberlain, 2015).

In Figure 1B we compare the Bonneville and Provo shoreline scaling relationships with two other estimates. Previously, Matsubara and Howard (2009) produced a spatially explicit model of the Great Basin and specifically analyzed the Bonneville region (see their Figures 4 and 5). Using their hydrologic modeling simulations Matsubara and Howard (2009) report an empirically derived multiplicative precipitation equation expressing precipitation factor change ( $P/P_M$ ) as a linear relationship with temperature depression ( $\Delta T$ ), where  $P/P_M = 2.2 + 0.2 \times \Delta T$  (orange line in Figure 1B), a steeper slope than those derived using our approach (Table 1). In a similar fashion Quirk and others (2018) recently reported relationships for LGM and post-LGM glacier extents in the Wasatch range (shown as black lines in Figure 1B). Most significantly, our

relationships for the Bonneville and Provo shorelines intercept the time-equivalent post-LGM relationships from Quirk and others (2018) at a precipitation factor change of  $\sim 1.2$  to 1.3 and a temperature depression of  $\sim 7$  °C, comparable to the median value from the macrofossil estimates reported by Harbert and Nixon (2018) and in agreement with the PMIP climate model ensemble average temperature depression of  $7.5^{\circ}\text{C}$  ( $\pm 2.6$ ,  $1\sigma$ ;  $n = 15$ ) for Lake Bonneville determined previously by Oster and others (2015).

## **CONCLUSIONS**

In sum, we have downscaled the scaling analysis presented by Ibarra and others (2018) for the western United States for the Bonneville and Provo shoreline areas of Lake Bonneville during the last glacial period. These estimates are similar to previous hydrologic modeling and glacier mass balance modeling efforts. Future work will also constrain the scaling relationships associated with the pre-LGM Stansbury shoreline and post-Bonneville Gilbert episode. Furthermore, ongoing work to constrain changes in surface and lake temperature using pollen, macrofossil and carbonate clumped isotopic techniques (e.g., Mering, 2015; Harbert and Nixon, 2018) will provide independent constraints on the regional magnitude of temperature depressions for the last glacial period. Finally, we anticipate that future more advanced spatially explicit hydrologic modeling (e.g., Matsubara and Howard, 2009; Barth and others, 2016; Hatchett and others, 2018) and isotope mass balance approaches (e.g., Ibarra and others, 2014; Hudson and others, 2017) for the Bonneville basin will provide inter-comparison between different methods for determining past changes in hydroclimate from lake area extents.

## **ACKNOWLEDGEMENTS**

Ibarra acknowledges Christine Y. Chen (MIT-WHOI), Robert S. Harbert (Stonehill College), Lauren M. Santi, Alexandra Arnold, Juan Lora (UCLA), Kate Maher and Tyler J. Kukla (Stanford University) for discussions and suggestions. NCEP Reanalysis data provided by the NOAA/OAR/ESRL PSD, Boulder, Colorado, USA, from their website at <https://www.esrl.noaa.gov/psd/>. Code used to generate Figure 1 can be obtained from Ibarra. This work was supported by National Science Foundation grant EAR-1450357 and the Heising-Simons Foundation to Chamberlain.



## REFERENCES

- Adams, K.D., and Bills, B.G., 2016, Chapter 8. Isostatic rebound and palinspastic restoration of the Bonneville and Provo shorelines in the Bonneville basin, UT, NV, and ID, in: Oviatt, C.G., Shroder Jr., J.F., editors, *Lake Bonneville: A Scientific Update*, v. 20. p. 145–164.
- Barth, C., Boyle, D.P., Hatchett, B.J., Bassett, S.D., Garner, C.B., and Adams, K.D., 2016, Late Pleistocene climate inferences from a water balance model of Jakes Valley, Nevada (USA): *Journal of Paleolimnology*, v. 56, p. 109–122 (doi: 10.1007/s10933-016-9897-z).
- Benson, L.V., Currey, D.R., Dorn, R.I., Lajoie, K.R., Oviatt, C.G., Robinson, S.W., Smith, G.I., and Stine, S., 1990, Chronology of expansion and contraction of four great Basin lake systems during the past 35,000 years: *Palaeogeography, Palaeoclimatology, Palaeoecology*, v. 78, p. 241–286 (doi: 10.1016/0031-0182(90)90217-U).
- Broecker, W., 2010, Long-term water prospects in the Western United States: *Journal of Climate*, v. 23, p. 6669–6683 (doi: 10.1175/2010JCLI3780.1).
- Budyko, M.I., 1974, *Climate and Life*. International Geophysical Series, v. 18.
- Chen, C.Y., and Maloof, A.C., 2017, Revisiting the deformed high shoreline of Lake Bonneville: *Quaternary Science Reviews*, v. 159, p. 169–189 (doi: 10.1016/j.quascirev.2016.12.019).
- Fu, B.P., 1981, On the calculation of the evaporation from land surface. *Sci. Atmos. Sin.*, v. 5, no. 1, p. 23–31.
- Gilbert, G.K., 1890, *Lake Bonneville*: U.S. Geological Survey Monograph, v. 1, p. 438.
- Grayson, D., 2011, *The Great Basin: a natural prehistory*: University of California Press, 432 p.
- Greve, P., Gudmundsson, L., Orlowsky, B., and Seneviratne, S.I., 2015, Introducing a probabilistic Budyko framework: *Geophysical Research Letters*, v. 42, p. 2261–2269 (doi: 10.1002/2015GL063449).
- Harbert, R., and Nixon, K., 2018, Quantitative Late Quaternary climate reconstruction from plant macrofossil proxy in Western North America: bioRxiv preprint, 17 p. (doi: 10.1101/340208).
- Hatchett, B.J., Boyle, D.P., Garner, C.B., Kaplan, M.L., Bassett, S.D., and Putnam, A.E., 2018, Sensitivity of a western Great Basin terminal lake to winter northeast Pacific storm track activity and moisture transport, in: Starratt, S.W., and Rosen, M.R., editors, *From Saline to Freshwater: The Diversity of Western Lakes in Space and Time*: Geological Society of America Special Papers, v. 536, 13 p. (doi: 10.1130/2018/2536(05)).
- Hostetler, S.W., and Benson, L.V., 1990, Paleoclimatic implications of the high stand of Lake Lahontan derived from models of evaporation and lake level: *Climate Dynamics*, v. 4, p. 207–217 (doi: 10.1007/BF00209522).
- Hubbs, C.L., and Miller, R.R., 1948, The zoological evidence: Correlation between fish distribution and hydro- graphic history in the desert basins of western United States, *in* *The Great Basin with emphasis on glacial and postglacial times*: Bulletin of the University of Utah, v. 38, no. 20, p. 17–166.
- Hudson, A.M., and Quade, J., 2013, Long-term east-west asymmetry in monsoon rainfall on the Tibetan Plateau: *Geology*, v. 41, p. 351–354 (doi: 10.1130/G33837.1).
- Hudson, A.M., Quade, J., Ali, G., Boyle, D., Bassett, S., Huntington, K.W., Marie, G., Cohen, A.S., Lin, K. and Wang, X., 2017, Stable C, O and clumped isotope systematics and <sup>14</sup>C geochronology of carbonates from the Quaternary Chewaucan closed-basin lake system, Great Basin, USA: Implications for paleoenvironmental reconstructions using carbonates: *Geochimica et Cosmochimica Acta*, v. 212, p. 274–302 (doi: 10.1016/j.gca.2017.06.024).

- Ibarra, D.E., Egger, A.E., Weaver, K.L., Harris, C.R., and Maher, K., 2014, Rise and fall of late Pleistocene pluvial lakes in response to reduced evaporation and precipitation: Evidence from Lake Surprise, California: *Geological Society of America Bulletin*, v. 126, p. 1387–1415 (doi: 10.1130/B31014.1).
- Ibarra, D.E., and Chamberlain, C.P., 2015, Quantifying closed-basin lake temperature and hydrology by inversion of oxygen isotope and trace element paleoclimate records: *American Journal of Science*, v. 315, no. 9, p. 781-808 (doi: 10.2475/09.2015.01).
- Ibarra, D.E., Oster, J.L., Winnick, M.J., Caves Rugenstein, J.K., Bryne, M.P., and Chamberlain, C.P., 2018, Warm and cold wet states in the western United States during the Pliocene-Pleistocene: *Geology*, v. 46, p. 355-358 (doi: 10.1130/G39962.1).
- Lora, J.M., Mitchell, J.L., Risi, C., and Tripathi, A.E., 2017, North Pacific atmospheric rivers and their influence on western North America at the Last Glacial Maximum: *Geophysical Research Letters*, v. 44, p. 1051–1059 (doi: 10.1002/2016GL071541).
- Maher, K., Ibarra, D.E., Oster, J.L., Miller, D.M., Redwine, J.L., Reheis, M.C., and Harden, J.W., 2014, Uranium isotopes in soils as a proxy for past infiltration and precipitation across the western United States: *American Journal of Science*, v. 314, p. 821–857 (doi: 10.2475/04.2014.01).
- Matsubara, Y., and Howard, A.D., 2009, A spatially explicit model of runoff, evaporation, and lake extent: Application to modern and late Pleistocene lakes in the Great Basin region, western United States: *Water Resources Research*, v. 45, p. W06425 (doi: 10.1029/2007WR005953).
- McGee, D., Quade, J., Edwards, R.L., Broecker, W.S., Cheng, H., Reiners, P.W., and Evenson, N., 2012, Lacustrine cave carbonates: Novel archives of paleo- hydrologic change in the Bonneville Basin (Utah, USA): *Earth and Planetary Science Letters*, v. 351, p. 182–194 (doi: 10.1016/j.epsl.2012.07.019).
- Mering, J.A., 2015, New constraints on water temperature at Lake Bonneville from carbonate clumped isotopes: University of California Los Angeles, M.S. thesis, 176 p.
- Mifflin, M.D., and Wheat, M.M., 1979, Pluvial lakes and estimated pluvial climates of Nevada: *Nevada Bureau of Mines and Geology Bulletin*, v. 95, 57 p.
- Miller, D.M., Oviatt, C.G., and McGeehin, J.P., 2013, Stratigraphy and chronology of Provo shoreline deposits and lake-level implications, late Pleistocene Lake Bonneville, eastern Great Basin, USA: *Boreas*, v. 42, p. 342–361 (doi: 10.1111/j.1502-3885.2012.00297.x).
- Orme, A.R., 2008, Pleistocene pluvial lakes of the American West: A short history of research: *Geological Society, London, Special Publications*, v. 301, p. 51–78 (doi: 10.1144/SP301.4).
- Oviatt, C.G., 2015, Chronology of Lake Bonneville, 30,000 to 10,000 yr B.P.: *Quaternary Science Reviews*, v. 110, p. 166-171 (doi: 10.1016/j.quascirev.2014.12.016).
- Oviatt, C.G., Habiger, G.D., and Hay, J.E., 1994, Variations in the composition of Lake Bonneville marl: a potential key to lake-level fluctuations and paleoclimate: *Journal of Paleolimnology*, v. 11, p. 19-30 (doi: 10.1007/BF00683268).
- Oster, J.L., Ibarra, D.E., Winnick, M.J., and Maher, K., 2015, Steering of westerly storms over western North America at the Last Glacial Maximum: *Nature Geoscience*, v. 8, p. 201–205 (doi: 10.1038/ngeo2365).
- Quirk, B.J., Moore, J.R., Laabs, B.J.C., Caffee, M.W., and Plummer, M.A., 2018, Termination II, Last Glacial Maximum, and Lateglacial chronologies and paleoclimate from Big

- Cottonwood Canyon, Wasatch Mountains, Utah: Geological Society of America Bulletin, 14 p. (doi: 10.1130/B31967.1).
- Reheis, M.C., 1999a, Extent of Pleistocene Lakes in the Western Great Basin: U.S. Geological Survey Miscellaneous Field Studies Map MF-2323, scale 1:800,000, 1 sheet.
- Reheis, M., 1999b, Highest pluvial-lake shorelines and Pleistocene climate of the western Great Basin: Quaternary Research, v. 52, p. 196–205 (doi: 10.1006/qres.1999.2064).
- Reheis, M.C., Adams, K.D., Oviatt, C.G., and Bacon, S.N., 2014, Pluvial lakes in the Great Basin of the western United States—a view from the outcrop: Quaternary Science Reviews, v. 97, p. 33–57 (doi: 10.1016/j.quascirev.2014.04.012).
- Roderick, M.L., Sun, F., Lim, W.H., and Farquhar, G.D., 2014, A general framework for understanding the response of the water cycle to global warming over land and ocean: Hydrology and Earth System Sciences, v. 18, p. 1575–1589 (doi: 10.5194/hess-18-1575-2014).
- Russell, I.C., 1885, Geological history of Lake Lahontan: a Quaternary lake of northwestern Nevada: U.S. Geological Survey Monograph, v. 11, 288 p.
- Williams, T.R., and Bedinger, M.S., 1984, Selected geologic and hydrologic characteristics of the Basin and Range Province, western United States; Pleistocene lakes and marshes: IMAP 1522-D, scale 1:2,500,000, 1 sheet.